2015 ASIA-PACIFIC SOLAR RESEARCH CONFERENCE

Peer Reviewed
2015 Solar Research Conference

A validated simulation of wind flow around a parabolic dish

Muhammad Uzair[1], Timothy Anderson[1], Roy Nates[1], and Etienne Jouin[2]

[1]*School of Engineering, Auckland University of Technology, Auckland, New Zealand*

[2]*Energy and Environmental Engineering Department, INSA Lyon, Lyon, France*

E-mail: timothy.anderson@aut.ac.nz

Abstract

The thermal performance of solar parabolic dish systems is greatly influenced by the wind around the system. To achieve higher operating temperatures, larger dish structures are used to increase the concentration ratio, however, the air flow around the structure affects the convective heat loss from the receiver. Previous studies investigating the effect of heat losses from the cavity receiver have treated it as a separate entity decoupled from the reflector. However, the interaction between wind and the dish structure can affect the local air speed at the cavity inlet and thus the heat loss as well.

In order to investigate the flow behavior, a three dimensional computational fluid dynamics (CFD) model was used to predict the steady-state flow around the parabolic solar dish at different operating conditions. The CFD model was subsequently validated with experimental data collected from wind tunnel testing for the dish at different pitch angles and with varying wind speeds. The results support the assertion that the flow characteristics near the cavity receiver aperture depend strongly on the orientation of the dish structure and this needs to be taken into account when analyzing the performance of parabolic dish systems.

1. Introduction

Concentrating solar power (CSP) systems can be classified into four main types; parabolic dish systems, solar towers, and parabolic troughs and Fresnel reflectors. Among these classifications, parabolic dish systems are considered to be the most efficient as a result of them achieving higher concentration ratios than the other techniques (Steinfield, 2004 and Tyner et al., 2001). To compete with conventional power generation techniques, the thermal performance of these CSP systems plays an important role. The performance of a CSP system utilizing a parabolic dish approach is sensitive to heat losses from the cavity receiver employed in these systems, particularly at high temperature. In particular, the heat loss from the cavity receiver is affected by the surrounding turbulent air, and consequently exposure to this results in increased heat loss, and the thermal performance decreases (Lupfert et al., 2001). Analytical techniques are available to determine the radiation and conduction heat losses from cavity receiver, however due to the complicated velocity and temperature field around the receiver, determination of convective heat losses is much more complicated.

Several previous experimental and analytical studies investigating the effect of convective heat loss from solar concentrator receivers have treated it as a separate entity, decoupled from the dish/reflector structure of a real parabolic dish system (Abbasi-Shavazia et al., 2014 and Reddy et al., 2015). However, the interaction between the wind and the dish structure can affect the local air speed at the cavity inlet and thus the heat loss as well.

Surprisingly there is a marked absence of research on the impact of the dish structure on the flow near the receiver and thus the performance of parabolic dish solar power systems. In one study, Paitoonsurikarn and Lovegrove (2006) numerically examined the local wind velocities near the cavity receiver in the presence of dish structure. They found that the local wind speed at the aperture was largest when the free stream wind flow was parallel to the aperture plane. Christo (2012) numerically investigated the transient flow behavior around the dish with regard to dust deposition on the dish surface, while most recently Uzair et. al., (2014) computationally investigated the effect of the dish structure on the heat loss from the receiver. In this regard, the present study, aims to further work of Uzair et. al., (2014) by computationally examining the wind flow around a parabolic dish and validating it experimentally.

2. Methodology

2.1. Numerical Setup

Following on from the work of Uzair et al (2014), the optical geometry of the Australian National University's 20 m^2 dish was selected as the basis of a three dimensional computational fluid dynamics (CFD) analysis of the air flow behavior around a 1:33 scale model of this dish in a wind tunnel. To undertake this analysis a commercial finite volume CFD solver, ANSYS CFX 15, was used. As the aim of the study was to simulate the air flow around a parabolic dish system, at a scaled down size, the dimensions and conditions of the wind tunnel experiment (discussed in the next section) were utilized to represent the extent of the computational domain.

A mesh sensitivity analysis was performed resulting in a highly refined mesh, of approximately 4.7 million elements, being used to perform a steady state simulation of the flow around the dish. As the flow around the dish was primarily turbulent, the shear stress transport (SST) turbulence model was used to resolve the flow, as this has been shown to accurately predict flow seperation and has been successfully used for studies of wind flow over parabolic troughs (Paetzold et al., 2014). The simulations were performed by changing the tilt angle of the dish relative to the wind from 90° to -90° with a free stream wind velocity of 3.2 m/s at a temperature of 20°C. The parabolic dish system was treated as a smooth wall as were the walls of the wind tunnel.

2.2. Experimental Setup

To validate the computational results, wind tunnel experiments were performed using a scaled model with an aperture diameter of 150mm, which could be used to analyze the flow behavior around dish. In order to get a smooth finish a nylon model of the dish model was manufactured using a three dimensional printing system. The model was mounted on a stand in the test section by means of 180mm long steel rod that allowed for rotation around the z-axis. A honeycomb structure was mounted at the inlet of wind tunnel to provide a streamlined flow. The test section around dish was 500 mm x 500mm in cross section, and extended 500mm upstream and 1000mm downstream of the model. After testing of the wind tunnel to ensure homogenous flow, it was decided to perform experiments qualitatively to study the flow pattern with smoke visualization to compare with computational results.

In order to diffuse the smoke in parallel lines inside the wind tunnel, a smoke rake was used. The flow visualization was captured in the presence of a green laser light sheet by a digital SLR camera. A schematic representation of the experimental setup is shown in Fig 1.

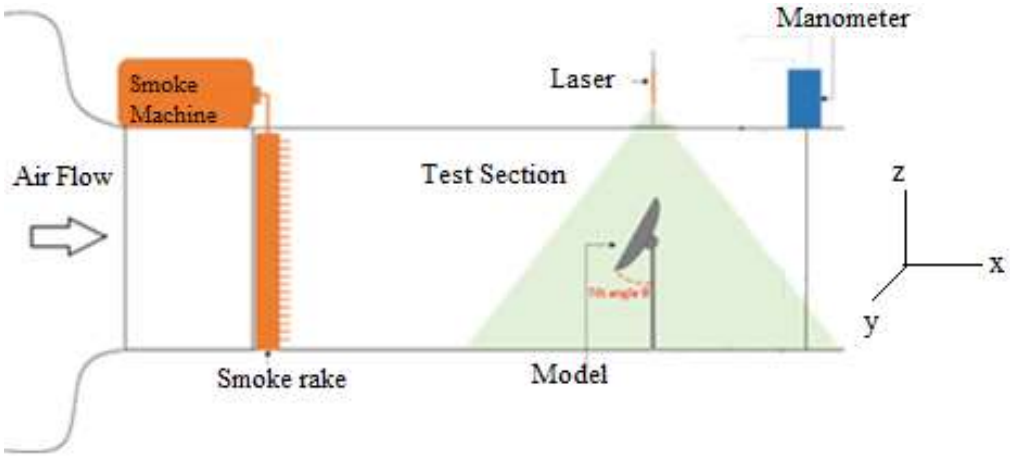

Fig 1: Schematic drawing of the experimental bench

3. Results and discussion

3.1. Qualitative Results

Three dimensional calculations were performed for the scaled model of the parabolic dish system at different pitch angles ranging from 90° (wind directly impinging on the reflective surface) to -90° (wind impinging on the rear of the dish). Detailed flow visualization around the parabolic dish structure was performed using smoke allowing the simulation results to be verified qualitatively. At different tilt angles of the dish velocity streamlines along the center plane of the virtual tunnels are shown in Fig. 2-6 with flow moving from left to right with the streamlines compared with the smoke visualization streak lines.

The flow field around the dish structure shows markedly different flow structures with different tilt angles. Starting from a case when flow is perpendicular to aperture plane of dish, i.e. 90° tilt angle; an accumulation of smoke in the front panel of the dish can be seen in Fig. 2. This is due to the dish structure blocking the horizontal movement of air, hence the local velocity becomes normal to the original flow near the dish corners. In turn the velocity in the front of the dish structure moves towards a stagnation condition and at the edges of the dish structure the velocity values increase to maintain continuity. As a result, the velocity behind the dish is reduced and two strong recirculating vortices are generated due to the reduced pressure in the dish's wake.

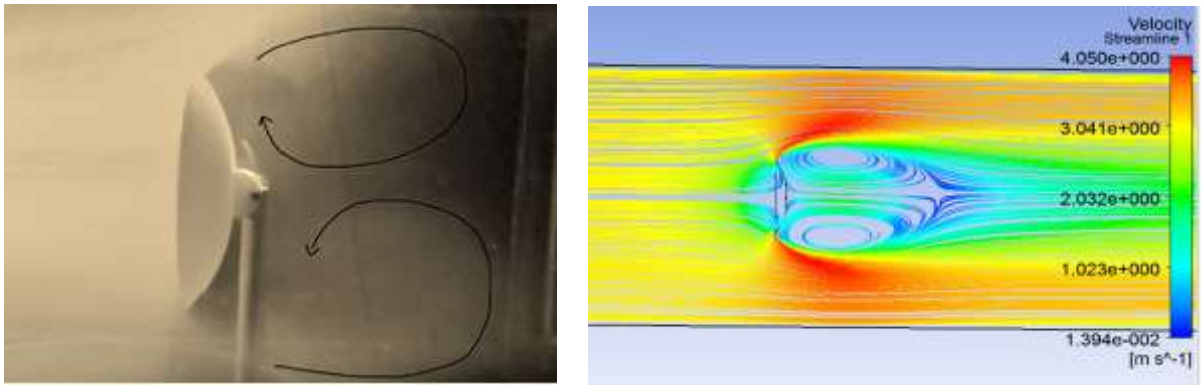

Fig 2: Flow visualization and stream lines for 90° tilt angle

By changing the tilt angle to 60°, the negative pressure creates flow separation at the upper and lower edge of the dish, resulting in two large rotating vortices behind the dish. From the velocity streamlines shown in Fig 3, it can be seen that the velocity magnitude increases at the upper

and lower edge, and this leads towards a flow separation. Similarly, Fig 4 shows flow separation occurring from the upper edges thus creating a vortex behind the dish at a pitch angle of 45°.

However as the angle is reduced further, to a tilt angle of 30°, the flow becomes more uniform without any major flow separation except a smaller flow recirculation region near to the lower portion of the dish, as shown in Fig. 5. As a result, there is no clear stagnation zone behind the dish, and the flow orientation is mainly upward due to the low pressure generated by the acceleration of the flow over the dish. The recirculation regions diminish as the dish approaches a zero degree tilt angle i.e. facing vertically upward and when the aperture plane is parallel to the flow, and it suggests that the dish does not affect the air flow on the top side of the dish for this orientation. Under these conditions, the receiver location would be in such a position that the shape of the dish would not impact the flow near it (Fig. 6).

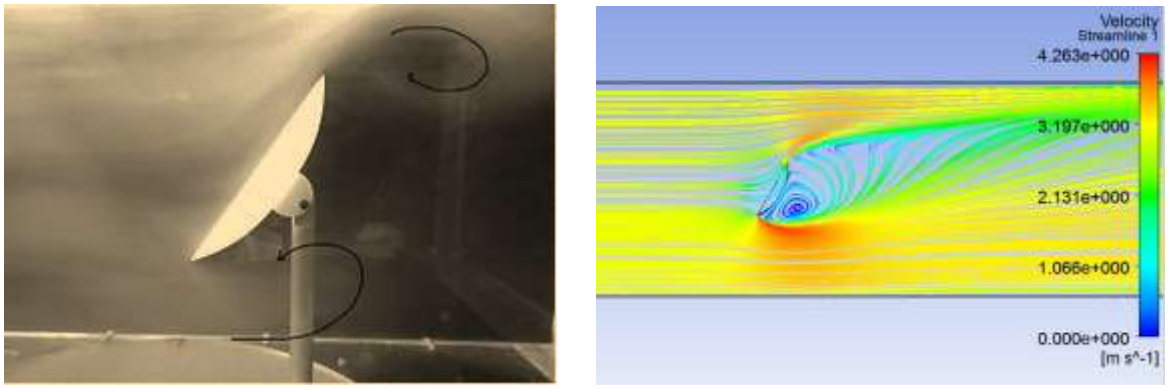

Fig 3: Flow visualization and stream lines for 60° tilt angle

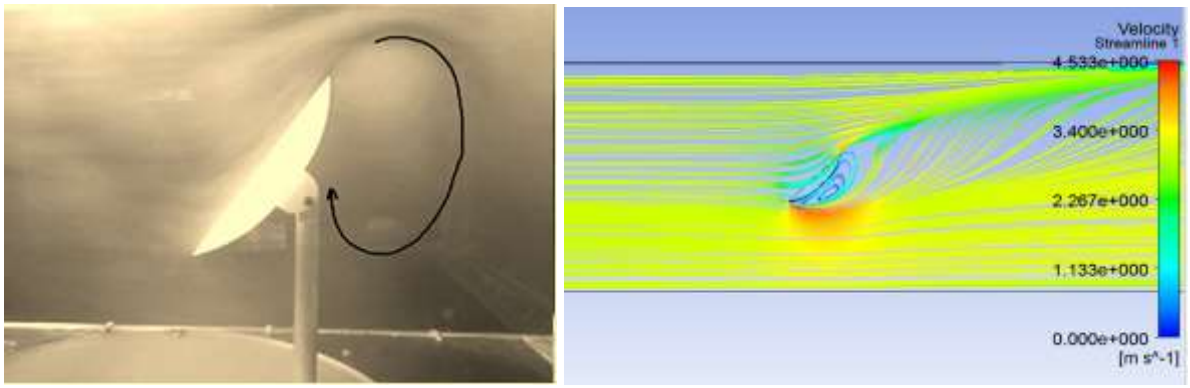

Fig 4: Flow visualization and stream lines for 45° tilt angle

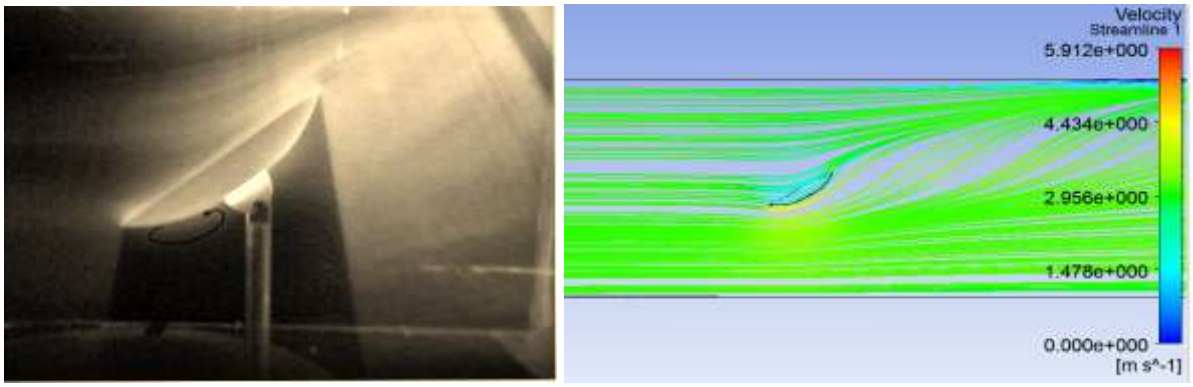

Fig 5: Flow visualization and stream lines for 30° tilt angle

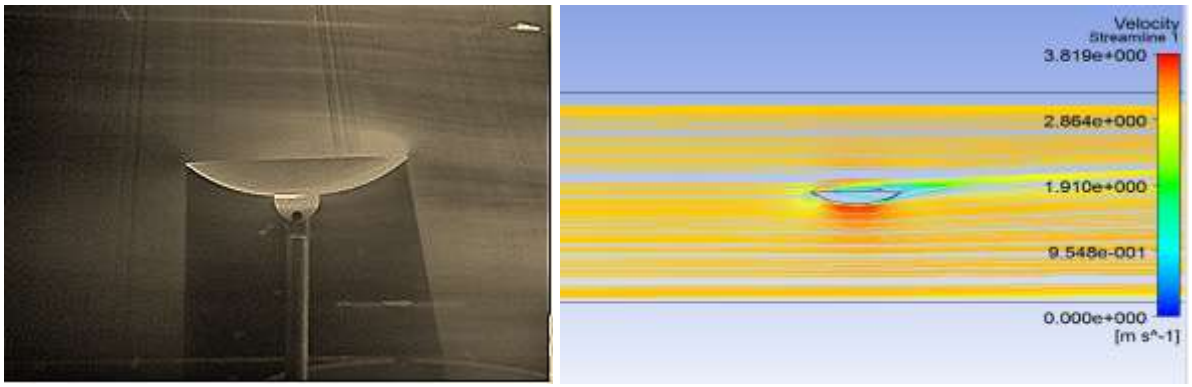

Fig 6: Flow visualization and stream lines for 0° tilt angle

Now, by changing the tilt angle to -30°, such that the flow is from the back side of the dish structure, the dish creates a strong vortex zone in its wake. As is visible in Fig 7, smoke becomes trapped behind the dish and rotates locally. This smoke cloud is especially visible when the smoke generation is stopped, and it takes a significant amount of time to disappear, thus illustrating that the air in this area is highly stagnant. Thus the local velocity is slow, and it is important to note that this is the area in which the cavity receiver would be, which suggests that for this orientation natural convection heat loss would be significant, whereas for other orientations the forced component might be dominant.

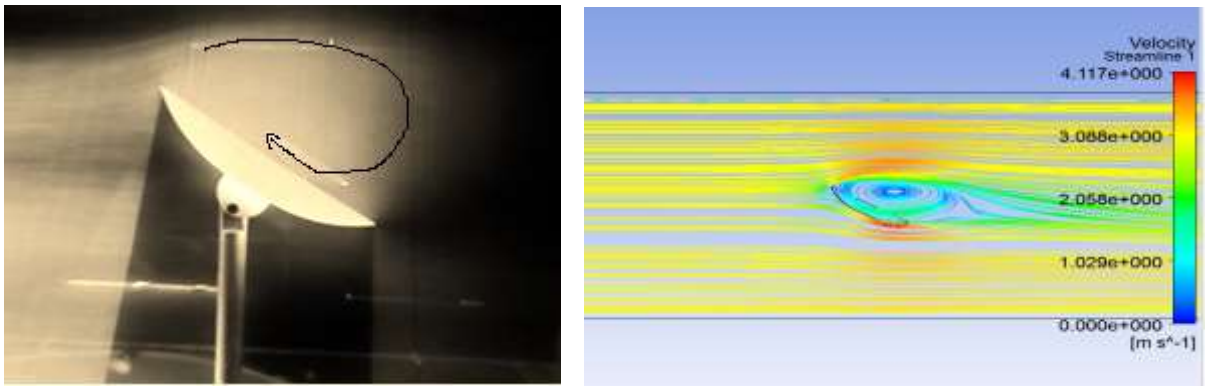

Fig 7: Flow visualization and stream lines for -30° tilt angle

By increasing the tilt angle to -45°, again a large recirculation can be viewed in the wake region of the dish which creates a disorderly air flow in this area, while a small recirculation can be viewed near the lower edge (Fig. 8). Similar to -30° tilt angle, the local flow velocity behind the dish structure reduces markedly. Now from the flow patterns, it can be observed that the flows near the aperture are dominated by the tangential components from 45° to -45° tilt angle. Fig 9 shows the flow pattern for a tilt angle of -60°, showing the high velocities at the edges of dish structure producing a negative pressure in the vicinity of the wake region. The negative pressure generates strong vortices behind the dish and like a 90° tilt angle, the circulation region increases sharply at a tilt angle of -90° generating two large vortices behind the dish structure (Fig. 10).

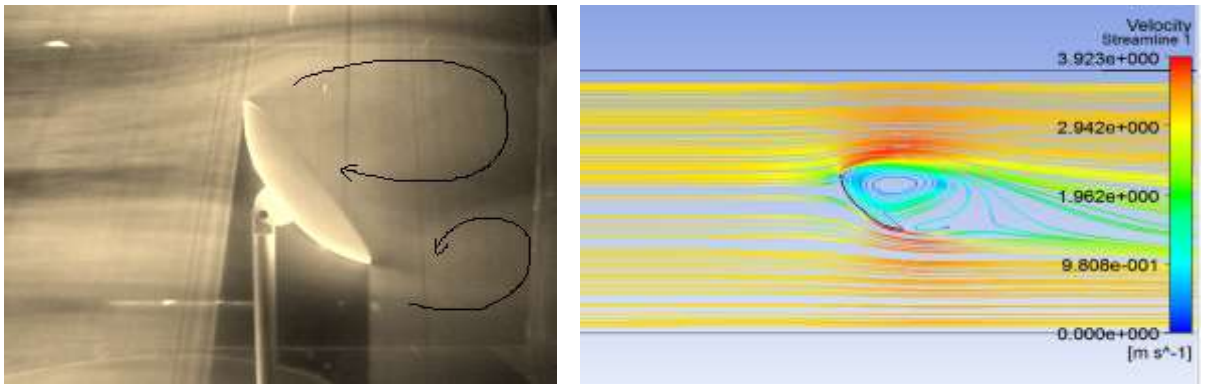

Fig 8: Flow visualization and stream lines for -45° tilt angle

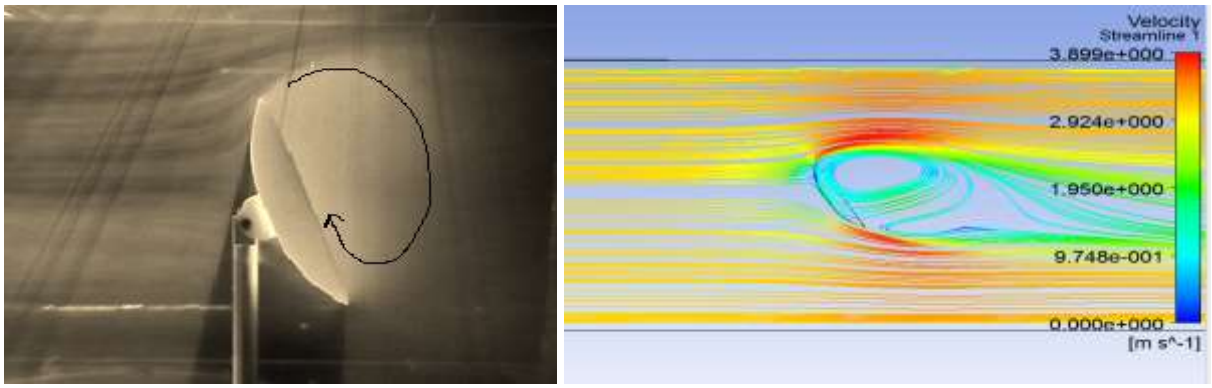

Fig 9: Flow visualization and stream lines for -60° tilt angle

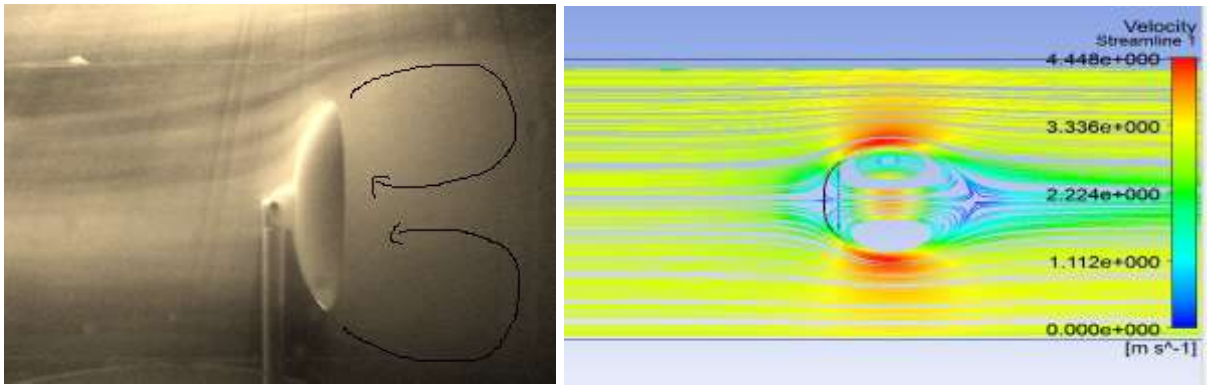

Fig 10: Flow visualization and stream lines for -90° tilt angle

3.2. Quantitative results

In examining these images the streaks of the flow stream illustrate a shear layer that can also be observed from the simulation results. It can be clearly seen that the shear layer's trajectory is totally dependent on the tilt angle of the dish structure. In turn, the shear layer disturbance at the edge of the dish structure defines the drag acting on the dish. It is observed that the maximum disturbance in the shear layer is in the case of a 90° tilt angle, when the flow is approaching perpendicular to the aperture plane of the dish from the front side. The disturbance of the shear layer reduces with a decreasing tilt angle, and it can be observed that the minimum shear layer disruption is the case of 0° tilt angle, when the aperture plane of the dish is facing vertically upward. The increase in the shear layer by increasing tilt angle can also be visualized with the air flow from the back side of dish.

Based on these observations, the drag coefficients were determined from the steady state simulations. The results showed that the drag coefficient was greatly influenced by the tilt angle. Fig. 11 compares the predicted drag coefficient values from this simulation with the analytical expression proposed by Christo (2012) and the experimental results presented by Wagner (1996). For this study the drag coefficient values were found to correspond well with those of these previous two studies. They show that the parabolic dish has a maximum drag coefficient when air flow approaches perpendicular to the aperture plane of the dish from the front side i.e. at 90° tilt angle. By changing the tilt angle, the drag coefficient decreases and a minimum value can be observed for a case when the dish aperture is facing vertically upward (0° tilt angle). The drag coefficient again increases by changing the tilt angle from 0° to -90° but the value remains lower than at a 90° tilt angle.

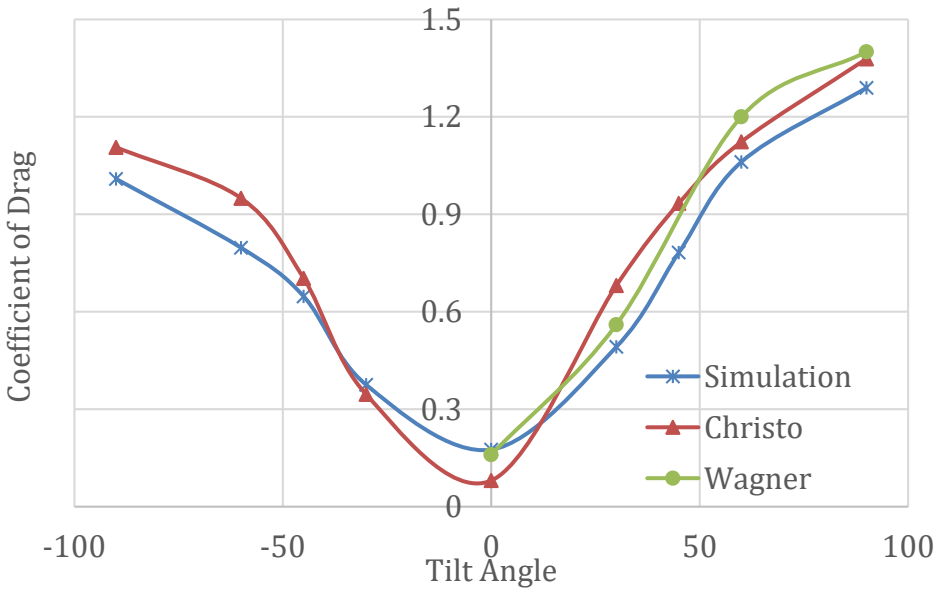

Fig 11: Comparison of drag coefficient at different tilt angles

In summary it can be seen that the flow predicted using computational fluid dynamics correlates both qualitatively with the experiments and quantitatively with the reported data in the literature. On this basis, it would appear that the use of CFD in the determination of heat losses from dish receivers holds significant promise.

4. Conclusion

This study has shown good agreement between quantitative and qualitative assessments of the flow field around a parabolic dish. The results indicate a significant disturbance to the local air velocities at all tilt angles, except in the case of flow parallel to the aperture of the dish. Moreover, it has demonstrated that the dish structure significantly impacts the flow, as quantified by the drag coefficients, and that the tangential component of the local wind speed at the aperture plane becomes dominant in most of the cases.

Based on these results, it can be concluded that the orientation of a parabolic dish has a significant effect on the local air velocity near the dish and consequently the air velocities near their cavity receivers. These velocity disturbances and recirculation areas near where the cavity receiver would be located would affect the heat losses and subsequently the overall performance of the parabolic dish concentrator. As such there is a need for further consideration of wind flow around parabolic dishes and the influence this will have on heat losses in the design of parabolic dish CSP systems.

References

Abbasi-Shavazia, E., Hughesb, G. O., Pye, J. D., 2014, 'Investigation of heat loss from a solar cavity receiver', *Energy Procedia*, 69, p269-278.

Ansys Inc. 2013, *CFX User guide*, ANSYS, Canonsburg

Christo, F., 2012, 'Numerical modelling of wind and dust pattern around a full-scale paraboloidal solar dish', *Renewable Energy*, 32, p356-366.

Paetzold J., Cochard C., Fletcher D., Vassallo A., 2014, 'Wind flow around parabolic trough solar collectors- A parametric study for optimisation of wind forces and heat losses', *Proceedings of Solar 2014*, Melbourne, Australia

Paitoonsurikarn, S., Lovegrove, K., 2006, 'Effect of paraboloidal dish structure on the wind near a cavity receiver', *Proceedings of the 44th Annual Conference of the Australian and New Zealand Solar Energy Society*, Canberra, September, 2006

Price, H., Lupfert, E., Kearney, D., 2002, 'Advances in Parabolic Trough Solar Power', *Journal of Solar Energy Engineering*, 124 (2), p109–126.

Reddy, K.S., Srihari, V. T., Veershetty G., 2015, 'Combined heat loss analysis of solar parabolic dish – modified cavity receiver for superheated steam generation', *Solar Energy*, 121, p78–93

Steinfield, A., 2005, 'Solar thermochemical production of hydrogen-a review', *Solar Energy*, 78, p603-615.

Tyner, CE., Kolb, GJ., Geyer, M., Romero, M., 2001, '*Concentrating solar power in 2001- an IEA/Solar PACES summary of present status and future prospectus'*, Solar PACES, www.solarpaces.org (Last cited 05/09/2015).

Uzair, M., Anderson, T., Nates, R., 2014, 'Wind Flow around a Parabolic Dish Solar Concentrator', *Proceedings of the 2014 Asia-Pacific Solar Research Conference*, Sydney, December 2014

Wagner, G.L., 1996, *Solar Concentrator Wind Loadings*, MSc Thesis, Texas Tech University